NUMERICAL ANALYSIS OF OPPOSED ROWS OF COOLANT JETS INJECTED INTO A HEATED CROSSFLOW

F. Bazdidi Tehrani   &   H. Feizollahi

Abstract: *The mixing characteristics of coolant air jets with the hot gas exiting the gas turbine combustor's primary zone is of major importance to the combustor exit temperature profile. In the present work, a three dimensional numerical simulation on the basis of the finite volume method was developed. The aim was to investigate the penetration and mixing characteristics of directly opposed rows of coolant jets injected normally into a heated confined cross stream. The ability of the standard and the realizable κ-ε turbulence models in the prediction of formation of dimensionless temperature profiles, downstream of jets, was evaluated. The effect of jet-to-mainstream momentum flux ratio, in the lower and upper limits of 25.0 and 60.0, at a fixed channel height-to-hole diameter ratio of 12.5 and a periodic distance of adjacent jets of 2 cm, was investigated. Also the effect of periodic distance in the range of 1-3 cm on the temperature profile was studied. Comparisons between the present numerical results on the temperature profiles and the experimental data of Wittig et al. [13] demonstrated reasonable agreement.*

1. Introduction

Mixing of an injected jet with a crossing stream is a three-dimensional phenomenon. This issue in the case of interaction of opposed jets, is further emphasized. The penetration and mixing characteristics of opposed coolant jets with the hot gas in the dilution zone of a gas turbine combustor are of major influence on the shape of temperature profile at the combustor's outlet. This profile has an important role in the determination of life cycle of turbine blades and hence it must conform well to blade stress levels.

Many workers have studied the characteristics of mixing and penetration of coolant jets injected into a heated confined crossflow, some of whom have begun their work with a single jet and then expanded it to opposed jets. Among the earlier works, Sridhara [1], Holdeman et al. [2] and Cox [3] carried out experimental and analytical investigations on multiple-jet configurations. Later on, Holdeman and walker [4] and Liscinsky et al. [5, 6] studied experimentally the normal injection of coolant jets in a rectangular duct.

They measured the dimensionless temperature profile at various axial positions from the jet origin and it was expressed as the mixing parameter, $(T_g - T_i)/(T_g - T_j)$ (T_j = jet inlet temperature, T_g = main flow temperature, T_i= local temperature).

Doerr et al. [7, 8] analyzed the mixing process in a rectangular duct for the jet-to-mainstream momentum flux ratio, J, beyond common values at J equal to 100 and 200 ($J = (\rho_j U_j^2)/(\rho_\infty U_\infty^2)$ where U_j and U_∞ = jet and mainstream inlet velocities, ρ_j and ρ_∞= jet and mainstream densities). They studied the optimized mixing and penetration and reported that at J values beyond those specified, an impingement of opposed jets would occur. More recently, Holdeman and Chang [9] focused on the effect of independently preheating the jet and main air in a cylindrical duct and the effect of varying the number of orifices with both the jet and main air preheated to the same temperature. The number of orifices was found to have a significant effect on mixing. Tao et al. [10] studied numerically the relationship between the temperature trajectory and the upstream flow and geometric variables in a row of jets discharging normally into a confined cylindrical crossflow. Lakehal [11] showed that turbulent Prandtl number has a considerable effect on the accurate prediction of turbulent convective heat transport in the cooling of gas turbine hot sections such as turbine blades. Bazdidi-Tehrani et al. [12] investigated

numerically the effect of both geometrical and flow variables on the temperature profile for a single row of jets injected normally into a confined crossflow. Wittig et al. [13] and Liscinsky et al. [14] did both experimental and numerical studies of the dimensionless temperature profile for directly opposed rows of coolant jets injected into a heated crossflow. Holdeman et al. [15] summarized available experimental and computational results on the mixing of opposed rows with the confined subsonic crossflow in rectangular ducts.

In the present work, the penetration and mixing characteristics of opposed rows of coolant jets injected normally into a heated confined cross stream in a rectangular duct and their influence on the formation of temperature profile have been studied numerically. Hence, the effect of both the flow and the geometrical variables has been investigated.

2. Governing Equations

The time-averaged equations governing the motion of an incompressible and compressible flow have been expressed in a general form, as follows [16]. The equation for conservation of mass, or the continuity equation, is defined as in Equation (1).

$$\frac{\partial \rho}{\partial t} + \nabla \cdot (\rho \vec{\upsilon}) = S_m \tag{1}$$

where, ρ is density, υ is velocity vector and S_m is the source term of mass added to the control volume.

The equation for conservation of momentum is given by:

$$\frac{\partial}{\partial t}(\rho \vec{\upsilon}) + \nabla \cdot (\rho \vec{\upsilon}\vec{\upsilon}) = -\nabla p + \nabla \cdot (\bar{\tau}) + \rho \vec{g} + \vec{F} \tag{2}$$

where, p, τ, ρg, and F are static pressure, stress tensor, gravitational body force and external body forces, respectively. F also contains other model-dependent source terms such as porous media and optional sources. The stress tensor τ is given by:

$$\bar{\tau} = \mu \left[\left(\nabla \vec{\upsilon} + \nabla \vec{\upsilon}^T \right) - \frac{2}{3} \nabla \cdot \vec{\upsilon} I \right] \tag{3}$$

where, μ is molecular viscosity, I is unit tensor, and the second term on the right hand side is the effect of volume dilation. The energy equation can be written as:

$$\frac{\partial}{\partial t}(\rho E) + \nabla \cdot (\vec{\upsilon}(\rho E + P)) = -\nabla \cdot (\sum_j h_j J_j) + S_h \tag{4}$$

where, S_h is energy source term.. The turbulent stresses τ are related to the velocity gradients via a turbulent viscosity, μ_t. This relationship is called the Boussinesq approximation [16]:

$$\tau_{ij} = -\rho \overline{u_i' u_j'} = \mu_t \left(\frac{\partial U_i}{\partial x_j} + \frac{\partial U_j}{\partial x_i} \right) - \frac{2}{3} \rho k \delta_{ij} \tag{5}$$

The proper choice of a turbulence model is of a great importance and it depends on many factors such as the flow physics, the required level of accuracy and the available computational resources. The standard κ-ε model [16] is a semi-empirical model based on model transport equations for the turbulence kinetic energy, κ, and its dissipation rate, ε. The turbulence kinetic energy and its rate of dissipation are obtained from the following transport equations:

$$\frac{\partial(\rho \kappa)}{\partial t} + div(\rho \kappa U) = div\left[(\mu + \frac{\mu_t}{\sigma_k})grad\ k\right] + G_\kappa + G_b \tag{6}$$
$$- \rho\varepsilon - Y_M + S_\kappa$$

$$\frac{\partial(\rho\varepsilon)}{\partial t} + div(\rho\varepsilon U) = div\left[(\mu + \frac{\mu_t}{\sigma_\varepsilon})grad\ \varepsilon\right] + C_{1\varepsilon}\frac{\varepsilon}{k}(G_\kappa + G_{3\varepsilon}G_b) \tag{7}$$
$$- C_{2\varepsilon}\rho\frac{\varepsilon^2}{k} + S_\varepsilon$$

In these equations, G_κ represents the generation of turbulence kinetic energy due to mean velocity gradients. G_b is the generation of turbulence kinetic energy due to buoyancy.

Y_M represents the contribution of the fluctuating dilatation in compressible turbulence to the overall dissipation rate. $G_{1\varepsilon}$, $G_{2\varepsilon}$ and $G_{3\varepsilon}$ are constants. σ_κ and σ_ε are the turbulent Prandtl numbers for κ and ε, respectively. S_κ and S_ε are optional source terms. The turbulent (or eddy) viscosity, μ_t, is computed by combining κ and ε, as in Equation (8):

$$\mu_t = \rho C_\mu \frac{k^2}{\varepsilon} \tag{8}$$

where, the model empirical constants $C_{1\varepsilon}$, $C_{2\varepsilon}$, C_μ, σ_κ and σ_ε have the following values:

$$C_{1\varepsilon} = 1.44, C_{2\varepsilon} = 1.92, C_\mu = 0.09,\ \sigma_k = 1.0,\ \sigma_\varepsilon = 1.3$$

Because of the limitations of the standard κ-ε in the modeling of C_μ and ε, the realizable κ-ε model, proposed by Shih et al. [17], was employed for studying the mixing characteristics of the opposed jets. This model is intended to address the deficiencies of traditional κ-ε models by adopting a new eddy-viscosity formula involving a variable C_μ and a new model equation for the dissipation rate, based on the dynamic equation of the mean-square vorticity fluctuations. The reader is referred to Shih et al. [17] for full details on the realizable κ-ε model.

3. Computational Domain

The present computational domain, as shown in Fig. 1, was selected according to the Wittig et al.'s [13]

experimental setup. In order to have a realistic velocity profile at the jet inlet, a plenum was considered. The relevant boundary conditions are outlined in section 6.
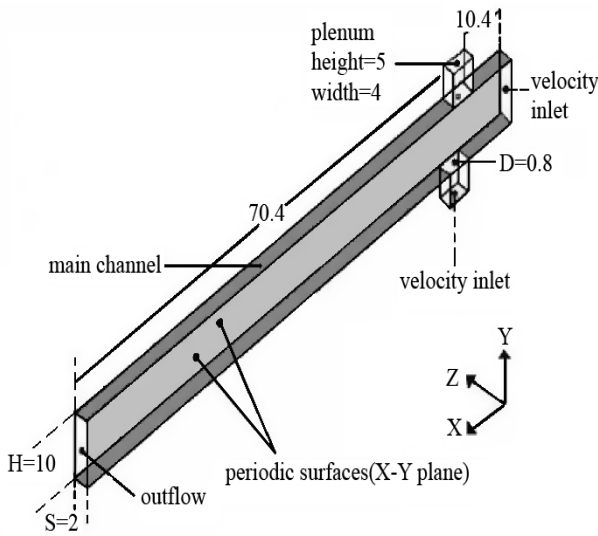

Fig. 1. Present computational domain (dimensions in cm)

4. Grid Generation

Computational fluid dynamics (CFD) methods, based on Cartesian or cylindrical coordinate systems, have certain limitations regarding irregular geometries [16], such as the geometry of a jet cross-section which is connected to a channel, as in the present work. Methods based on the body-fitted grid or the non-orthogonal grid systems, do not have such limitations and hence, in the present work, the body-fitted grid was used.

Four structured mesh sizes (hexahedral elements) were employed to verify the independence of present numerical solution from the mesh size. The finest and the coarsest grids were ($260 \times 80 \times 30$) and ($94 \times 20 \times 12$), respectively. Fig. 2 depicts a typical mesh generated comprising the top and bottom plenums of the geometry of the computational domain shown in Fig. 1. Similar to the work reported previously [12], the present numerical solution employed the finite volume based finite difference method [16, 18] and it included the following details: (1)

5. Numerical Details

Solution of the governing equations on the basis of three-dimensional Cartesian coordinates, with adaptive grids and variable density was employed. (2) The first and second order Upwind schemes were used to discretize the convection terms. (3) The SIMPLE algorithm was employed to correct the pressure term. (4) The standard κ-ε and realizable κ-ε models with standard wall functions were used. (5) The mixing was considered as a non-reacting flow. (6) The value of 1×10^{-7} was considered for the convergence criterion of the energy equation and 1×10^{-4} for the other equations.
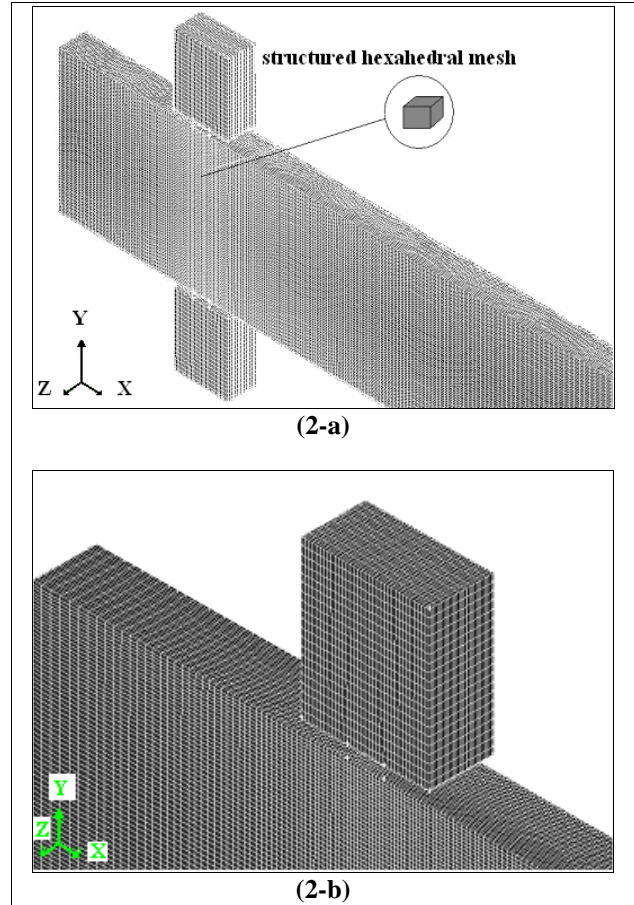

Fig. 2. Generated mesh (2-a) including top and bottom plenums and (2-b) mesh topology

6. Boundary Conditions

The computational domain, as represented by Fig. 1, had eight boundaries. An inlet and an outlet plane of the channel, two periodic planes, two inlet planes for the top and bottom plenums, and two solid walls at the top and bottom of domain. At the inlet boundaries, uniform profiles of velocity and temperature were specified from the experimental data [13]. Where, the relevant boundary conditions for two common limits of jet-to-mainstream momentum flux ratio, J, were chosen as follows:

(1) Lower limit of J:
$J_B = 24$ (at $U_{Bj} = 4.277$ m/s), $J_T = 25$ (at $U_{Tj} = 4.366$ m/s), $U_\infty = 18.4$ m/s, $T_\infty = 554.4$ K, $T_j = 316.3$ K, $S/D = 2.5$

(2) Upper limit of J:
$J_B = 60.24$ (at $U_{Bj} = 6.816$ m/s), $J_T = 57.8$ (at $U_{Tj} = 6.676$ m/s), $U_\infty = 18.5$ m/s, $T_\infty = 558.4$ K, $T_j = 318.7$ K, $S/D = 2.5$

where, subscripts Tj and Bj stand for top jet and bottom jet, but in this case U is velocity at the plenum entrance. In another word, all jets boundary conditions

were applied at the plenums entrances. Also, S is periodic distance of adjacent jets centers and D is jet hole diameter.

The turbulence intensity of mainstream and jets were set as 1% and 3%, respectively [16]. At the channel outlet, sufficiently far from the jets (7 times that of channel height), a zero gradient was considered as the boundary condition for all the variables, except the pressure (i.e., outflow boundary condition).

Due to jets being spread when injected into a crossflow, the side walls were assumed as periodic boundary conditions. On the periodic plane (X –Y plane), the inlet flux was equated to the outlet flux normal to the plane.

The top and bottom walls of channel and plenum planes were considered as adiabatic and the wall function method was employed [16]. The jet holes discharge coefficient, C_d, varied from 0.62 to 0.64 [19]. The results for the temperature field were presented as vertical profiles of the dimensionless temperature ratio, T/T_j , where, T is local temperature and T_j is jet static temperature.

The effect of periodic distance of adjacent jets on the penetration and mixing characteristics of opposed rows of jets was studied. Three values of S (S=1, S=2 and S=3cm) were considered and a comparison with the Holdeman equation [2] ($C = (S/H)\sqrt{J}$, where, H is channel height and C is a constant which is equal to 1.25 for opposed jets) was made. For this purpose, new values at the jets and mainstream boundaries were considered as:

$$U_{jB} = U_{jT} = 68 \ m/s, \ U_\infty = 18.4 \ m/s, \ T_\infty = 554.4 \ K, \ T_j = 316.3 \ K$$

In this particular case, all jets boundary conditions were applied at the jets inlets and not at the plenums entrances. The Holdeman equation, based on these new values, would give rise to an optimum value of S=1.51 cm.

7. Results

Fig. 3 represents the independence of present results on the temperature profile (T/T_j) from the mesh size at the lower limit of J and at X/H=0.5. In order to achieve a better accuracy, the finest grid (260 × 80 × 30) was used throughout the present study. The geometrical parameters H/D =12.5 and S/D =2.5 were kept constant, unless otherwise stated.

Fig. 4 illustrates that the variation of turbulence intensity of opposed jets in the range of 3-20 % in the lower limit of J and at X/H=0.5, had a little effect on the core of crossflow (Y/H=0), but a considerable effect (about 6 percent increase in T/T_j) for Y/H < - 0.2 and Y/H > 0.2.

Fig. 5 shows a comparison between the present numerical results, based on the standard and the realizable $κ$-$ε$ turbulence models, and the experimental results of Wittig et al. [13] in the lower limit of J and at

X/H=0.5. It can be seen that there was no distinct difference in the ability of the two models to predict the variations of T/T_j. Hence, due to a better convergence rate, the standard $κ$-$ε$ model was employed throughout the rest of the present work.
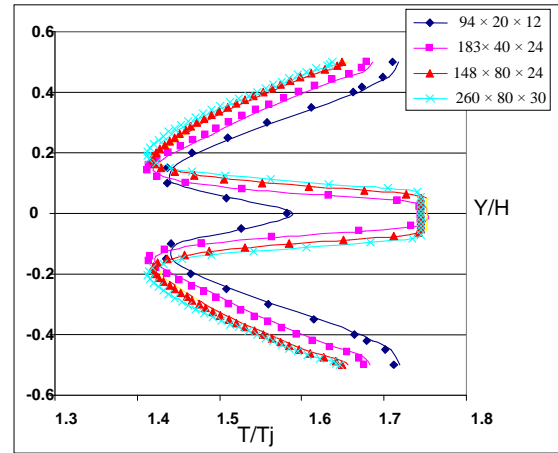

Fig. 3. Independence of present results on temperature profile from mesh size ($J_B = 24$, $J_T = 25$, X/H=0.5).
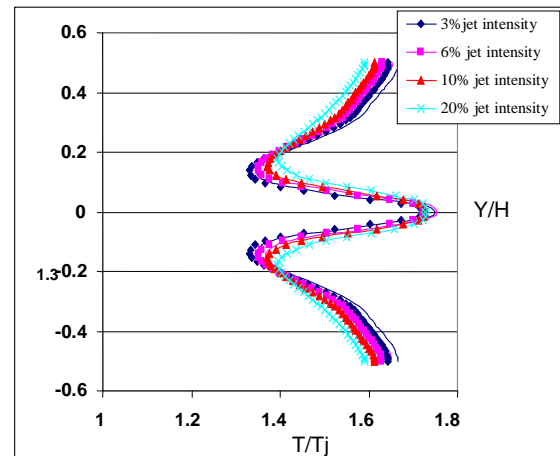

Fig. 4. Effect of turbulence intensity of opposed jets on temperature profile ($J_B = 24$, $J_T = 25$, X/H=0.5).

Fig. 6 demonstrates a comparison between the present results using the second order and first order Upwind schemes and the available experimental results of Wittig et al. [13]. The second order discretization scheme was employed so as to achieve a higher level of accuracy together with a smaller number of iterations. It can be noticed that the second order scheme predicted a lower jet penetration than that of the first order scheme, but as for the shape of temperature profile it provided a better consistency with the experimental results. A lower jet penetration, however, resulted in a stronger influence of cross stream (at Y/H=0.0) and hence a higher channel center-plane temperature relative to the jet temperature.
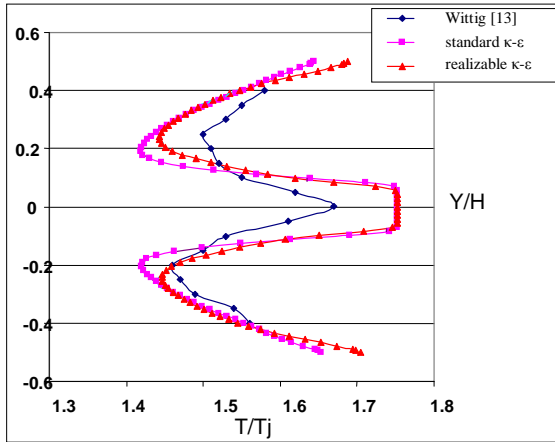
Fig. 5. Effect of turbulence models on temperature profile (J_B = 24, J_T = 25, X/H=0.5).
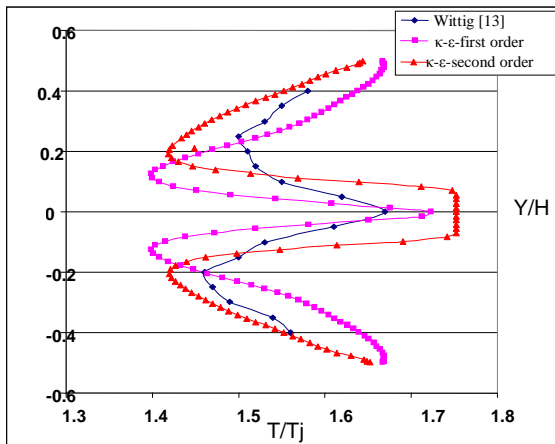

Fig. 6. Effect of first and second order Upwind schemes on temperature profile (J_B = 24, J_T = 25, X/H=0.5).

Fig. 7 shows the present temperature profiles in the lower limit of J at the jet center-line plane (*Z/S=0.0*) and for two different axial positions downstream of jet origin, *X/H=0.25* and *0.50*.

The agreement with the experimental results was overally acceptable, but an increase in X/H caused a slight increase in the relative difference, particularly at the core of crossflow. Similar results are presented by Fig. 8, where the lateral distance from jet center-line varied to *Z/S=0.4* (i.e. in the vicinity of periodic boundaries).

Fig. 9 illustrates the present temperature profiles in the upper limit of J at the axial position, *X/H=0.25*, and for two different lateral distances of *Z/S=0.0* and *0.4*. It can be seen that, as shown in the previous Figures, the second order scheme displayed a better consistency with the experimental results concerning the shape of temperature profile.
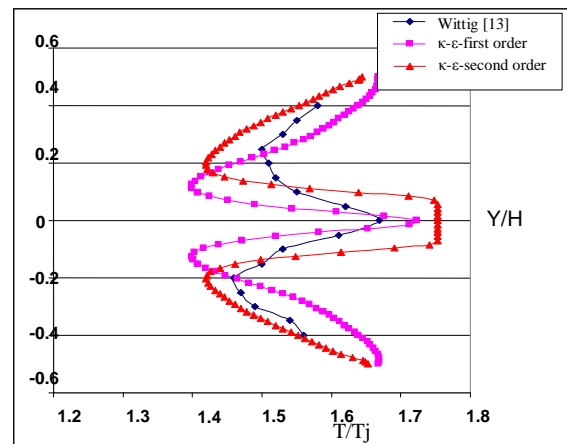
At *Z/S=0.4*, the first order scheme gave an unacceptable prediction of the shape of profile. Also an increase in the lateral distance to *Z/S=0.4* caused a

relative deviation of profile (almost 19 percent) in the core of crossflow.

A comparison of Fig. 7(a) with Fig. 9(a) shows an increase in the jet penetration as J was increased from the lower to the upper limit.
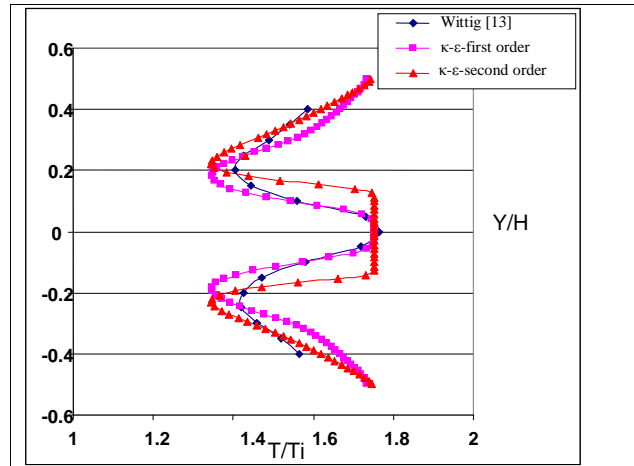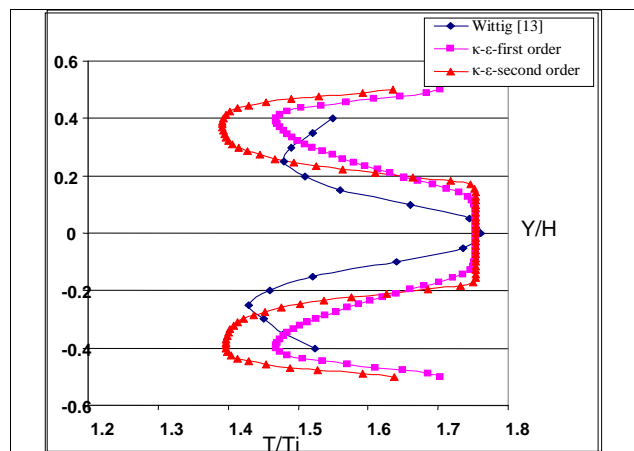

(7-a)

(7-b)

Fig. 7. Temperature profiles in the lower limit of J at *Z/S*=0.0 and for (7-a) *X/H*=0.25 and (7-b) *X/H*=0.50.
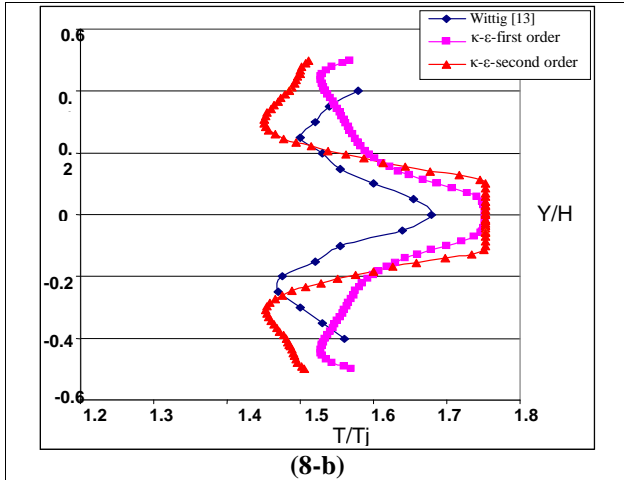

(8-a)

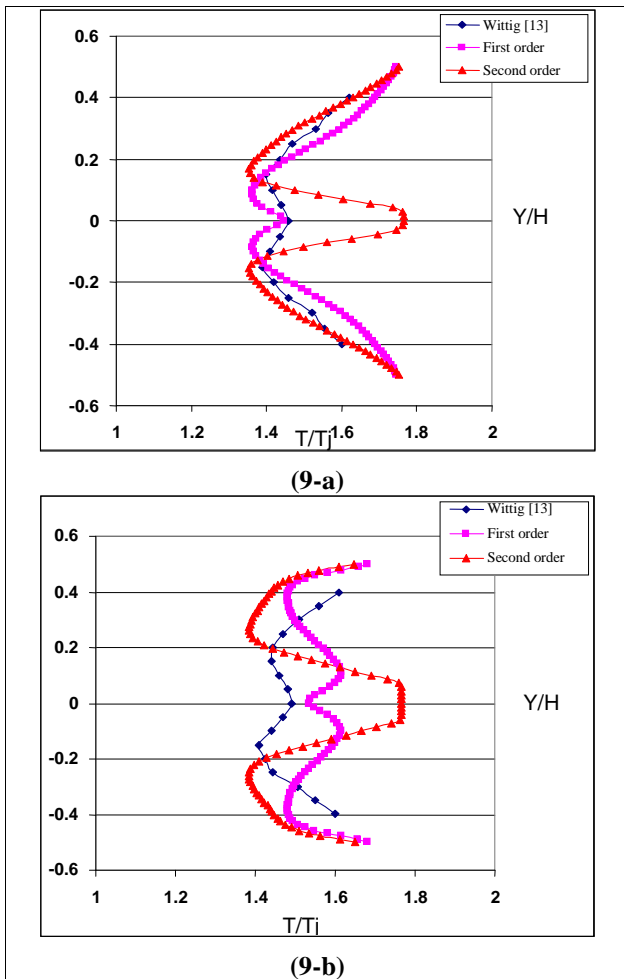**Fig. 8. Temperature profiles in the lower limit of J at** *Z/S=0.4* **and for (8-a)** *X/H=0.25* **and (8-b)** *X/H=0.50***.**

(9-a)

(9-b)

Fig. 9. Temperature profiles in the upper limit of J at *X/H=0.25* **and for (9-a)** *Z/S=0.0* **and (9-b)** *Z/S=0.4***.**

Fig. 10 represents the effect of variation of the periodic distance of adjacent jets centers, S, in the range of 1- 3 cm, on the temperature profile. This range was chosen to be close to an optimum value of *S=1.51* cm, which

was calculated using the Holdeman empirical equation. So far, a fixed value of *S=2* cm (*S/D=2.5*) was employed. It can be seen that an increase in *S* caused a higher jet penetration and hence a lower channel center- plane (*Y/H = 0.0*) temperature relative to the jet temperature. Also, this increase resulted in higher T/T$_j$ values at *Y/H < - 0.05* and *Y/H > 0.05* (i.e., towards the opposed jets origins), which are undesirable. The trends for *S=2* cm and *S=1.51* cm (optimum value) were quite close to one another.
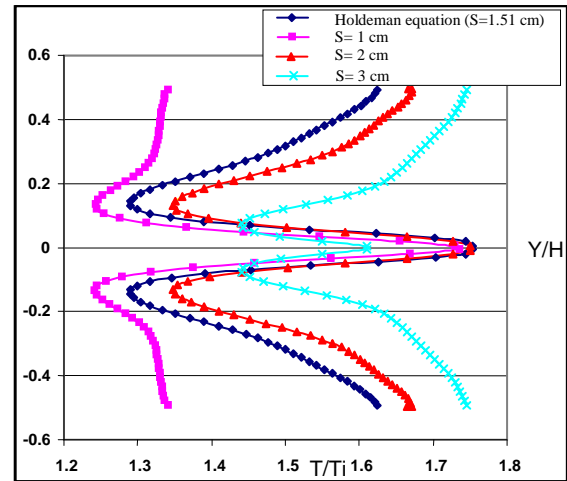

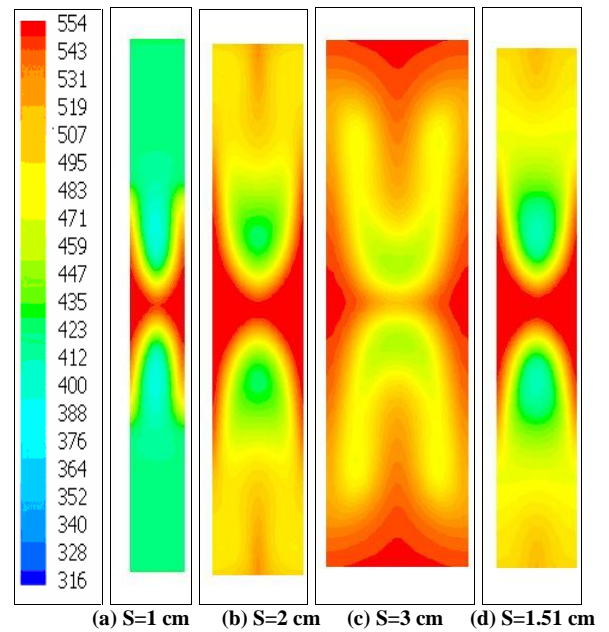**Fig. 10. Effect of variation of periodic distance on temperature profile (***Z/S=0.00, X/H=0.5, J=24***).**

(a) S=1 cm   (b) S=2 cm   (c) S=3 cm   (d) S=1.51 cm
Fig. 11. Temperature contours (Z -Y plane at *Z/S=0.0, X/H =0.5* **and** *J=24***).**

Fig. 11 displays the temperature contours in the form of lateral cross-section (Z-Y plane) for various values of S at *X/H=0.5*. These contours approve that increasing S would cause a higher jet penetration and also a stronger possibility of hot crossflow passing in between adjacent coolant jets.

This is further illustrated by Fig. 12 representing the temperature contours in the form of longitudinal cross-section (X-Z plane) for two values of S at Y/H= 0.2. The possibility of hot crossflow passing in between adjacent jets with an increase in S is clearly seen. Hence, an investigation of interaction of opposed jets should only be carried out three-dimensionally and also for various planes, if the true nature of mixing characteristics is to be discovered.
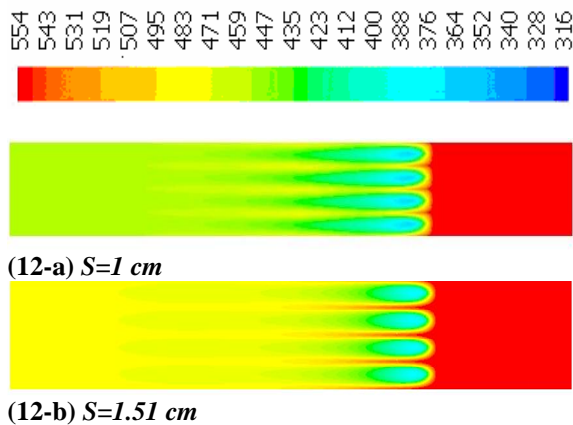

(12-a) *S=1 cm*

(12-b) *S=1.51 cm*

Fig. 12. Temperature contours (X-Z plane at Y/H=0.2 and J=24).

In order to propose an optimum design condition for the directly opposed rows of coolant jets, encountered in the dilution zone of an annular combustion chamber, further investigations need to be carried out. This could be accomplished by varying the geometrical parameters such as H/D and S/D (i.e., by changing D as well as S and H).

8. Conclusions

(1) An increase in the turbulence intensity of opposed jets showed a little effect on T/T_j at *Y/H=0.0*, but it caused a 6 % increase in T/T_j for *Y/H < - 0.2* and *Y/H > 0.2*.

(2) A comparison between the present results of two turbulence models with the experimental data of Wittig et al. [13] displayed no distinct difference in the ability of either to predict the variation of T/T_j. Hence, the standard κ-ε model was employed due to its better rate of convergence.

(3) The second order Upwind scheme predicted a lower jet penetration than that of the first order scheme, but as for the shape of the temperature profile it provided a better consistency with the experimental results for both limits of J.

(4) An increase in the value of J from the lower limit of 25 to the upper limit of 60 influenced the numerical accuracy significantly. For instance, the first order scheme gave an unacceptable prediction of the shape of temperature profile at *Z/S=0.4*. Also, a relative deviation of profile (almost 19 %) in the core of crossflow, at *Z/S=0.4*, was reported. Finally, an increase in jet penetration with J was demonstrated.

(5) Increasing the periodic distance of adjacent jets would cause a higher jet penetration and also a stronger possibility of hot crossflow passing in between adjacent jets.

(6) Further three-dimensional investigations on the geometrical parameters such as H/D and S/D need to be carried out before an optimum design condition for the opposed rows of jets could be proposed.

References

[1] Sridhara, K., *"Gas Mixing in the Dilution Zone of a Combustion Chamber"*, M.Sc. thesis 20/187, College of Aeronautics, Cranfield, England, 1967.

[2] Holdeman, J.D., Walker, R.E., Kors, D.L., *"Mixing of Multiple Dilution Jets With a Hot Primary Stream for Gas Turbine Combustors"*, NASA TM X-71426 (also AIAA Paper 73-1249, Ninth propulsion Conference, Las Vegas, 1973.

[3] Cox, G.B., *"An analytical model for Predicting Exit Temperature Profile From Gas Turbine Engine Annular Combustors"*, AIAA paper 75-1307, 1975.

[4] Holdeman, J.D., Walker, R.E., *"Mixing of a Row of Jets with a Confined Cross Flow"*, AIAA Journal, Vol. 15, No. 2, 1977, pp. 243-249.

[5] Liscinsky, D.S., True, B., Vranos, A., Holdeman, J.D., *"Experimental Study of Cross-Stream Mixing in a Rectangular Duct"*, Paper No. AIAA-92-3090, 1992.

[6] Liscinsky, D.S., True, B., Vranos, A., Holdeman, J.D., *"Experimental Investigation of Cross Flow Jet Mxing in a Rectangular Duct"*, Paper No. AIAA-93-3037, 1993.

[7] Doerr, T., Blomeyer, M., Hennecke, D.K., *"The Mixing Process in the Quenching Zone of Rich-Lean-Combustion Concept"*, Proc. 81st symposium on fuel and combustion technology for advanced aircraft engines, AGARD-PEP Fiuggi, 1993.

[8] Doerr, T., Blomeyer, M., Hennecke, D.K., "*Optimization of Multiple Jets Mixing with a Confined Crossflow*", J. Engrg. Gas Turbines Power, Vol. 119, 1997, pp. 315-321.

[9] Holdeman, J.D., Chang, C.T., *"The Effects of Air Preheat and Number of Orifices on flow and Emissions in an RQL Mixing Section"*, J. Fluids Engineering, Vol. 129, No. 11, 2007, pp. 1460–1467.

[10] Tao, Y., Adler, W., Spechr, E., *"Numerical Analysis of Multiple Jets Discharging Into a Confined Cylindrical Cross Flow"*, J. Process Mechanical Engineering, Vol. 216, Part E, 2002, pp. 173-180.

[11] Lakehal, D., *"Near-Wall Modeling of Turbulent Convective Heat Transport in Film Cooling of Turbine Blades with the Aid of Direct Numerical Simulation Data"*, J. Turbomachinery, Vol. 124, 2002, pp. 485-489.

[12] Bazdidi-Tehrani, F., Shahmir, A., Haghparast-Kashani, A., *"Numerical Analysis of a Single Row of Coolant Jets*

Injected Into a Heated Cross Flow", J. Computational and Applied Mathematics, Vol. 168, 2004, pp. 53-63.

[13] Wittig, S.L.K., Elbahar, O.M.F., Noll, B.E., *"Temperature Profile Development in Turbulent Mixing of Coolant Jets with a Confined Hot Cross Flow"*, J. Engrg. Gas Turbines Power, Vol. 106, 1984, pp. 193-197.

[14] Liscinsky, D.S., True, B., Vranos, A., Holdeman, J.D., "*Mixing Characteristics of Directly Opposed rows of Jets Injected Normal to a Cross Flow in a Rectangular Duct*", Paper No. AIAA-94-0217, 1994.

[15] Holdeman, J.D., Liscinsky, D.S., Bain, D.B*., "Mixing of Multiple Jets with a Confined Subsonic Cross Flow: part II-Opposed Rows of Orifices in Rectangular Ducts*", J. Engrg. Gas Turbines Power, Vol. 121, 1999, pp. 551-562.

[16] Versteeg, H.K., Malalasekera, W., *"An Introduction to Computational Fluid Dynamics: The Finite Volume Method*", Addison-Wesley, 1996.

[17] Shih, T.H., Liou, W.W., Shabbir, A., Yang, Z., Zhu, J., *"A new $\kappa - \varepsilon$ Eddy-Viscosity Model for High Reynolds Number Turbulent Flows - Model Development and Validation*", Computers Fluids, Vol. 24, 1995, pp. 227-238.

[18] Patankar, S.V., "*Numerical Heat Transfer and Fluid Flow"*, Hemisphere Publishing Corporation, Washington DC, 1980.

[19] Lefebvre, A.H., "*Gas Turbine Combustion"*, 2nd edition, McGraw-Hill, New York, 1999